fibers

MDPI

Article

Geometry of Chalcogenide Negative Curvature Fibers for CO_2 Laser Transmission

Chengli Wei [1], Curtis R. Menyuk [2] and Jonathan Hu [1,*]

[1] Department of Electrical and Computer Engineering, Baylor University, Waco, TX 76798, USA; cwei@umhb.edu

[2] Department of Computer Science and Electrical Engineering, University of Maryland Baltimore County, Baltimore, MD 21227, USA; menyuk@umbc.edu

* Correspondence: jonathan_hu@baylor.edu; Tel.: +1-254-710-1853

Received: 12 July 2018; Accepted: 27 September 2018; Published: 30 September 2018

Abstract: We study the impact of geometry on leakage loss in negative curvature fibers made with As_2Se_3 chalcogenide and As_2S_3 chalcogenide glasses for carbon dioxide (CO_2) laser transmission. The minimum leakage loss decreases when the core diameter increases both for fibers with six and for fibers with eight cladding tubes. The optimum gap corresponding to the minimum loss increases when the core diameter increases for negative curvature fibers with six cladding tubes. For negative curvature fibers with eight cladding tubes, the optimum gap is always less than 20 μm when the core diameter ranges from 300 μm to 500 μm. The influence of material loss on fiber loss is also studied. When material loss exceeds 10^2 dB/m, it dominates the fiber leakage loss for negative curvature fiber at a wavelength of 10.6 μm.

Keywords: CO_2 lasers; negative curvature fibers; chalcogenide glass; fiber loss; mid-IR

1. Introduction

Carbon dioxide (CO_2) lasers have been widely used in surgery, medicine, and material processing [1–3]. Step index fibers are commonly used to transmit CO_2 laser light. The material loss of silica glass in the mid-infrared limits the transmission of mid-infrared light using silica step-index fibers. However, it is possible in principle to obtain a lower loss in hollow-core fiber than in step-index fiber because air does not contribute to material loss [4,5]. In addition, the nonlinearity in the glass sets a limit to the transmitted power. Hollow-core fibers have low nonlinearity, because the light is mostly transmitted in air, which does not contribute to the nonlinearity. Recently, hollow-core negative curvature fibers have drawn a large amount of interest due to their attractive properties including low loss, broad bandwidth, and a high damage threshold [6–12]. The delivery of mid-infrared radiation has also been demonstrated using chalcogenide negative curvature fibers for a CO_2 laser at a wavelength of 10.6 μm [13–15]. Previous study shows that chalcogenide glass should be used for wavelength larger than 4.5 μm [16]. The relative simplicity of the negative curvature structure could enable the fabrication of fiber devices for mid-IR applications using non-silica glasses, such as chalcogenide [13–15].

The guiding mechanism in negative curvature fibers is inhibited coupling [10,17,18]. A large amount of research [10,19] has been carried out to determine the impact of fiber parameters on leakage loss [20] in negative curvature fibers and then optimize these parameters to minimize the loss. These parameters include the curvature of the core boundary, the thickness of the tubes, the number of cladding tubes, and the nested cladding tubes [17,18,21–24]. By introducing a gap between cladding tubes, the loss can be decreased in negative curvature fibers [24,25]. When the tubes touch, modes exist in the localized node area. A gap between the cladding tubes removes the additional resonances due to the localized node. Fibers with a gap between tubes are also expected to be easier to fabricate,

since surface tension would assist to maintain the circular shape of the tubes [22]. On the other hand, when the gap is too big, the core mode can leak through the gaps, which increases the loss in negative curvature fibers [26]. Therefore, an optimum gap exists. The optimal gap corresponding to the minimum loss in a fiber with six cladding tubes is three times as large as the optimal gap in fibers with eight or ten cladding tubes [26]. In a fiber with six cladding tubes, a larger gap is needed to remove the weak coupling between the core mode and tube modes [26].

In previous studies, the optimum gap was found in negative curvature fibers with a fixed core diameter [26]. Chalcogenide negative curvature fibers with different core diameters of 170 µm to 380 µm have been fabricated [13–15]. In this paper, we find optimal structures of chalcogenide negative curvature fibers for CO_2 laser transmission, in which we minimize the loss in the two-dimensional parameter space that consists of the core diameter and the gap size. In previous studies, the optimum gap was found in negative curvature fibers with a fixed core diameter [26]. We find that the minimum leakage loss decreases when the core diameter increases both for fibers with six and for fibers with eight cladding tubes. The optimum gap increases when the core diameter increases for negative curvature fibers with six cladding tubes. The optimum gap is always less than 20 µm when the core diameter increases for negative curvature fibers with eight cladding tubes when the core diameter ranges from 300 to 500 µm. We find optimal structures of chalcogenide negative curvature fibers for CO_2 laser transmission, in which we minimize the loss in the two-dimensional parameter space that consists of the core diameter and the gap size.

2. Geometry

Negative curvature fibers with six and eight cladding tubes have been fabricated by several research groups [17,25,27,28]. Figure 1 shows schematic illustrations of negative curvature fibers with six and eight cladding tubes. The white regions represent air, and the gray regions represent glass. The inner tube diameter, d_{tube}, the core diameter, D_{core}, the tube wall thickness, t, the minimum gap between the cladding tubes, g, and the number of tubes, p, are related by the expression: $D_{\text{core}} = (d_{\text{tube}} + 2t + g)/\sin(\pi/p) - (d_{\text{tube}} + 2t)$ [29]. We calculate the leakage loss for negative curvature fibers using Comsol Multiphysics, a commercial full-vector mode solver based on the finite-element method. Perfectly matched layers are added outside the cladding region in order to reduce the size of the simulation window [30]. The wavelength of 10.6 µm for a CO_2 laser is used in our simulation.

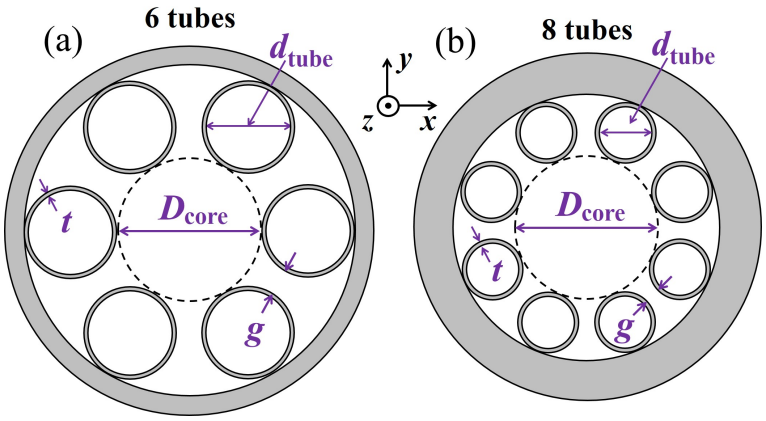

Figure 1. Schematic illustration of negative curvature fibers with (**a**) six and (**b**) eight cladding tubes.

3. As_2Se_3 Chalcogenide Glass

In this section, we study the loss in negative curvature fibers made with As_2Se_3 chalcogenide glass. We use a refractive index of 2.8 and a material loss of 10.6 dB/m for As_2Se_3 chalcogenide glass in our simulations [31]. The tube thickness, t, is fixed at 5.2 µm corresponding to the third antiresonance. A glass thickness corresponding to the third antiresonance has been drawn in the past [15]. A thicker

tube wall with a higher-order antiresonance makes fabrication easier. Geometries that use tube thicknesses corresponding to the first, second, or third antiresonance have similar minimum losses in the transmission band [16,26]. We first study negative curvature fibers with six cladding tubes. We define $d_{6\text{max}}$ as the maximum possible tube diameter for the fiber with 6 cladding tubes, which equals $D_{\text{core}} - 2t$. Figure 2a shows the contour plot of loss as a function of core diameter, D_{core}, and normalized tube diameter, $d_{\text{tube}}/d_{6\text{max}}$. For a fixed D_{core}, the loss decreases and then increases when $d_{\text{tube}}/d_{6\text{max}}$ increases from 0.2 to 1.0. The minimum loss occurs when $d_{\text{tube}}/d_{6\text{max}} = 0.62$, and it does not change when D_{core} increases from 300 to 500 μm. The loss decreases when D_{core} increases. In addition, we show the loss as a function of the core diameter, D_{core}, and the gap, g, in Figure 2b. The loss first decreases and then increases as the gap, g, increases. When there is no gap, a mode exists in the node that is created by the two touching tubes [25]. When the gap is too large, core mode leaks through the gap [17,26]. Previous study shows that the electric field intensity in the middle of the gap between cladding tubes can increase by a factor of 15 when the gap increases from 5 to 10 μm in a silica negative curvature fiber with a glass index of 1.45 and a core diameter of 30 μm at a wavelength of 1 μm [10]. Here, we study chalcogenide negative curvature fibers with a glass index of 2.8 at a wavelength of 10.6 μm. The electric field intensity in the middle of the gap between cladding tubes increases by a factor of 15 when the gap increases from 50 to 100 μm in a negative curvature fiber with a core diameter of 300 μm. We also plot the loss as a function of gap, g, for different core diameters in Figure 3a. In order to quantify the minimum loss and the corresponding optimum gap for different core diameters, we also plot the minimum loss and the corresponding optimum gap, g, using blue solid curve and red dashed curves, respectively, in Figure 3b. When the core diameter increases from 300 to 500 μm, the minimum loss decreases by more than one order of magnitude and the corresponding optimum gap, g, increases from 60 to 90 μm. Hence, a larger gap is needed for a fiber with a larger core diameter to decrease the loss in negative curvature fibers with six cladding tubes.

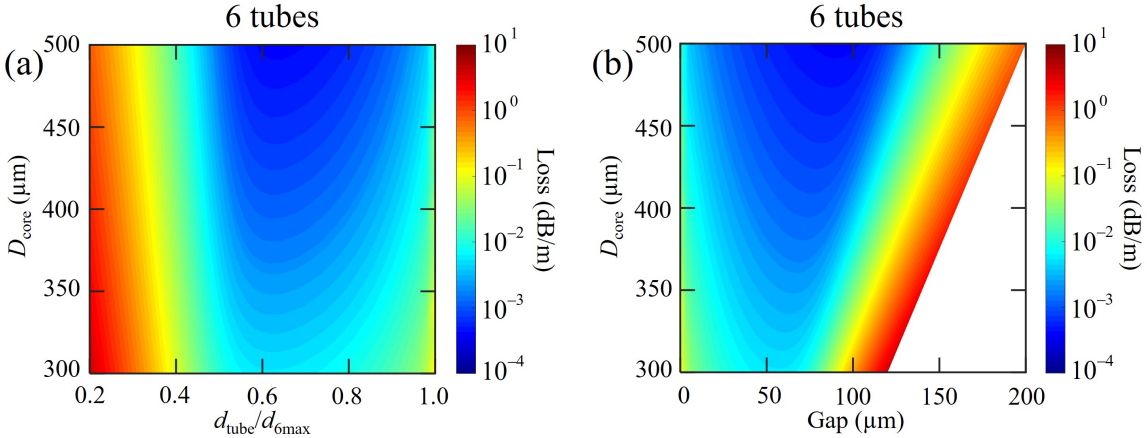

Figure 2. (**a**) Contour plot of loss as a function of core diameter and normalized tube diameter. (**b**) Contour plot of loss as a function of core diameter and gap. The number of cladding tubes is six.

We next carry out the same loss analysis on negative curvature fibers with eight cladding tubes. Figure 4a shows the contour plot of loss as a function of core diameter, D_{core}, and normalized tube diameter, $d_{\text{tube}}/d_{8\text{max}}$, where $d_{8\text{max}}$ is defined as the maximum possible tube diameter for the fiber with 8 cladding tubes, which is $D_{\text{core}}\sin(\pi/8)/[1-\sin(\pi/8)] - 2t$ [32]. Figure 4b shows the contour plot of loss as a function of core diameter, D_{core}, and gap, g. The minimum loss occurs at a larger value of $d_{\text{tube}}/d_{8\text{max}}$, or a smaller value of g, than is the case for negative curvature fibers with six cladding tubes. In Figure 5a, we show the loss as a function of the gap, g, for different core diameters. The optimum gap corresponding to the minimum loss is less than 20 μm for fibers with different core diameters and the loss increases slowly when gap further increases. The minimum loss and the corresponding gap, g, are plotted using blue solid curve and red dashed curves, respectively,

in Figure 5b. The minimum loss decreases by around one order of magnitude when the core diameter increases from 300 to 500 μm. Different from fibers with six cladding tubes, the corresponding optimum gap, g, is much smaller and is always less than 20 μm when the core diameter increases from 300 to 500 μm in fibers with eight cladding tubes. There is a wide range of gaps that realize low loss in the fibers with eight cladding tubes, as shown in Figure 5a. The loss is less sensitive to the gap in the region between 10 and 50 μm. Since the tube diameter is much smaller than the diameter of core, the coupling between the core mode and tube modes is weak. It has been shown that the power ratio in the air region of cladding tubes is always less than 0.1% in the negative curvature fiber with eight cladding tubes, while the power ratio in tube air could be more than 0.8% for fibers with six cladding tubes [26]. In negative curvature fibers with six cladding tubes, a larger gap is needed to remove the weak coupling between the core and cladding tube modes.

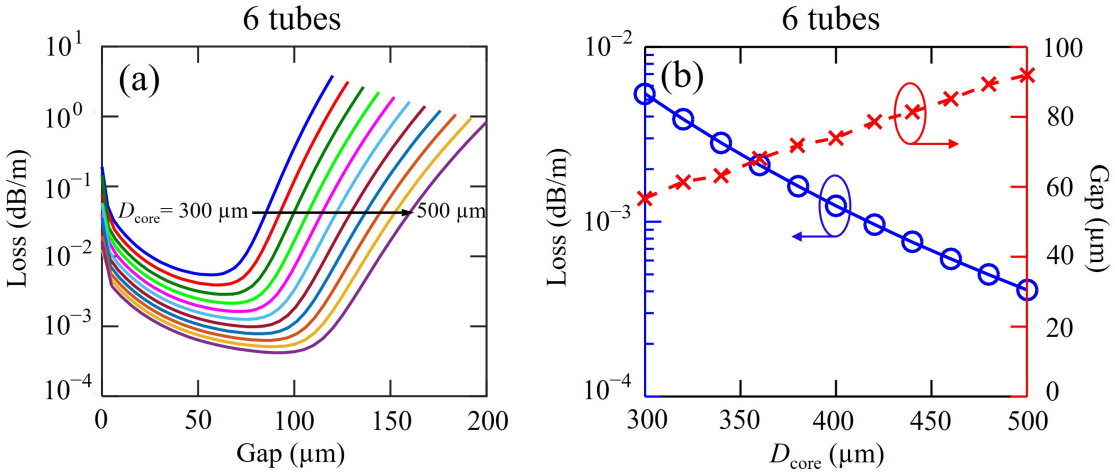

Figure 3. (**a**) Loss as a function of gap in fibers with different core diameters. (**b**) Minimum loss and the corresponding optimum gap in fibers with different core diameters. The number of cladding tubes is six.

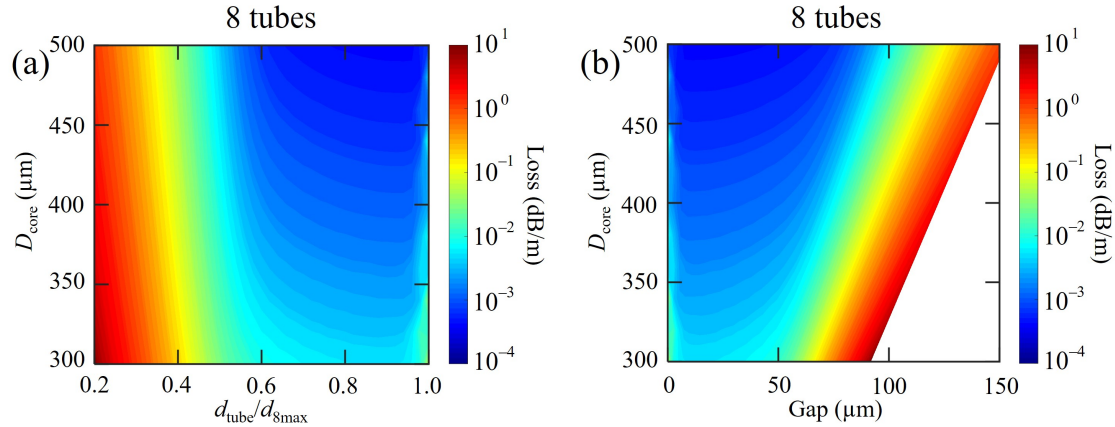

Figure 4. (**a**) Contour plot of loss as a function of core diameter and normalized tube diameter. (**b**) Contour plot of loss as a function of the core diameter and gap. The number of cladding tubes is eight.

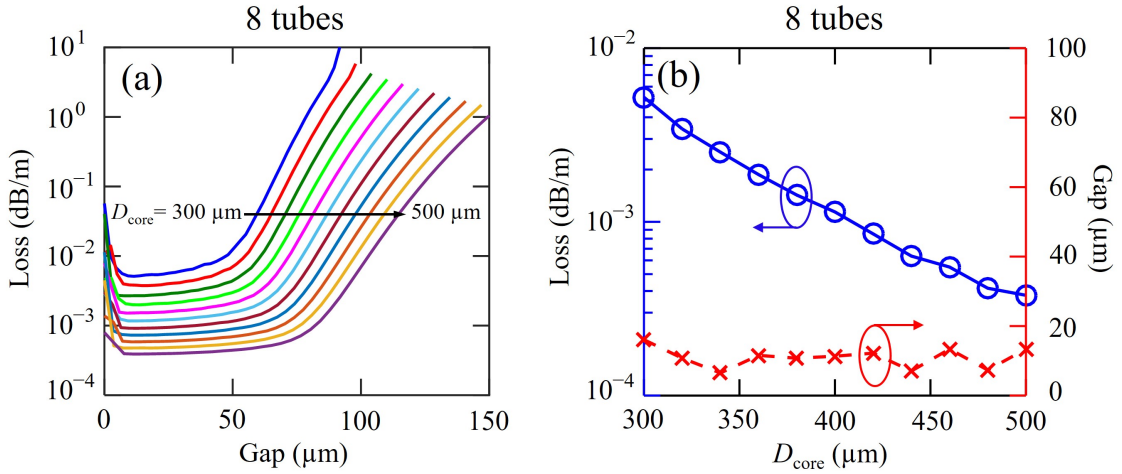

Figure 5. (**a**) Loss as a function of the gap in fibers with different core diameters. (**b**) Minimum loss and the corresponding gap in fibers with different core diameters. The number of cladding tubes is eight.

4. As_2S_3 Chalcogenide Glass

In this section, we carried out the same loss analysis in negative curvature fibers made with As_2S_3 chalcogenide glass. We use a refractive index of 2.4 and a material loss of 500 dB/m for As_2S_3 chalcogenide glass in our simulations [15,16]. The tube thickness, t, is fixed at 6.1 μm corresponding to the third antiresonance. Figure 6a shows the loss as a function of gap, g, when the core diameter increases from 300 to 500 μm in As_2S_3 chalcogenide fiber with six cladding tubes. Compared with the loss in Figure 3a, the losses in the fiber using As_2S_3 chalcogenide glass, shown in Figure 6a, are higher and have a flatter minimum. In Figure 6b, we show the minimum loss and the corresponding gap, g, as blue solid curve and red dashed curve, respectively. We also study the fiber leakage loss with and without material loss in an As_2S_3 chalcogenide fiber with six cladding tubes. In Figure 7a, we show the results in order to explain the broad, low-loss region in Figure 6a. The core diameter is fixed at 300 μm. The solid curve shows the fiber loss with material loss of 500 dB/m for As_2S_3 chalcogenide glass, which is the same as the blue solid curve in Figure 6a. The dashed curve shows the fiber loss without material loss, which is similar to the curve in Figure 3a. The high material loss of As_2S_3 chalcogenide glass dominates and leads to a flat minimum in the fiber loss curve, as shown by the blue solid curve in Figure 7a.

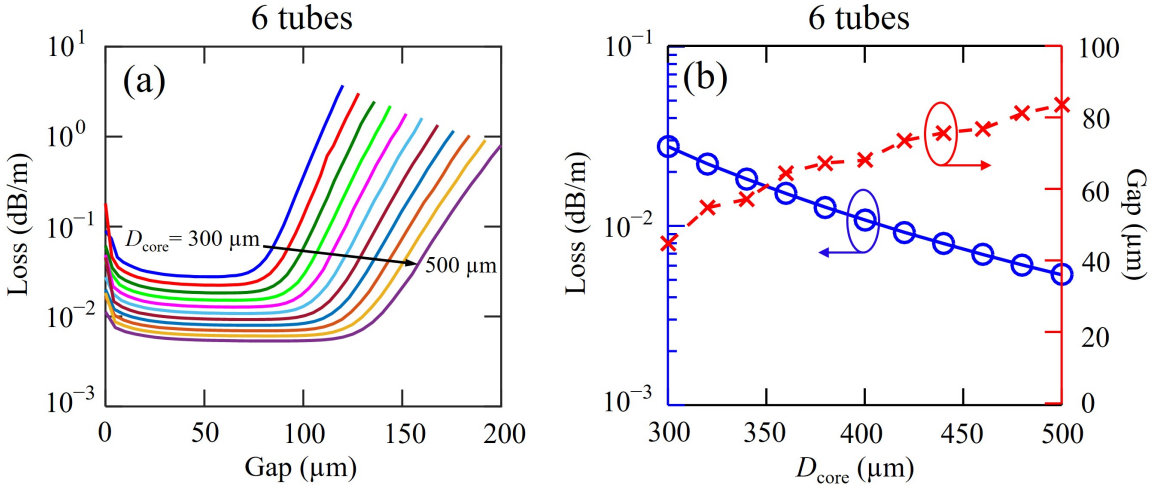

Figure 6. (**a**) Loss as a function of gap in fibers with different core diameters. (**b**) Minimum loss and corresponding optimum gap in fibers with different core diameters. There are six cladding tubes.

In order to better illustrate the influence of the material loss on the total fiber loss, we study the fiber loss as a function of material loss both for As_2S_3 chalcogenide glass and As_2Se_3 chalcogenide glass, shown in Figure 7b as the red dashed and blue solid curves, respectively. The core diameter is 300 μm and the gap is 60 μm. The fiber loss changes little when the material loss increases from 0.1 to 10 dB/m, and the fiber loss is dominated by the confinement loss in the blue region for both curves. The loss of fiber that is made with As_2Se_3 chalcogenide glass is located in the blue region, which is marked with the blue circle on the blue solid curve. The fiber loss begins to increase when the material loss increases from 10 to 10^2 dB/m, and the influence of the material loss becomes visible. When the material loss further increases, the fiber loss increases sharply, and the fiber loss is dominated by the material loss in the red region for both curves, when the material loss is higher than 10^2 dB/m. The loss of fiber made with As_2S_3 chalcogenide glass is located in the red region, which is marked with the red triangle on the red dashed curve. Due to the inhibited coupling between the core mode and glass modes, the power ratios in the glass of negative curvature fibers for the two points marked by circle and triangle in Figure 7b are 0.0016% and 0.002%, respectively. With this low power ratio in glass [33], the fiber leakage loss in negative curvature fibers is more than three orders of magnitude lower than the material loss of glass, as shown in Figure 7b.

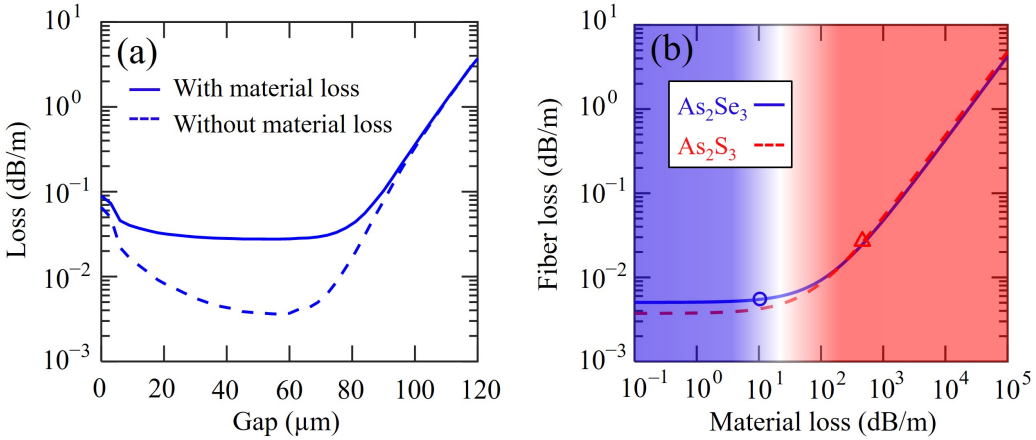

Figure 7. (**a**) Loss as a function of gap in fibers with and without material loss. (**b**) Fiber loss as a function of material loss in As_2Se_3 chalcogenide glass fiber and As_2S_3 chalcogenide glass fiber with six cladding tubes, a core diameter of 300 μm, and a gap of 60 μm.

Figure 8a shows the loss as a function of gap, g, in As_2S_3 chalcogenide fiber with eight cladding tubes. In Figure 8b, we show the minimum loss and the corresponding gap, g, using a blue solid curve and a red dashed curve, respectively. The minimum loss decreases by less than one order of magnitude and the corresponding optimum gap, g, is always less than 20 μm, which agrees with the results in the As_2Se_3 chalcogenide fiber with 8 cladding tubes. Small loss variation near zero gap occurs due to the glass modes existed near the node area between two tubes in Figure 8a.

Chalcogenide negative curvature fibers with eight cladding tubes have been successfully fabricated. The fiber loss was measured to be 2.1 dB/m at 10 μm for a fiber with a core diameter of 172 μm and a gap of 9 μm. Due to the structure distortion during fabrication, the losses of fabricated fibers are two orders of magnitude higher than the losses in simulation, indicating there are room to improve the fabrication [34]. The distortion of the negative curvature fiber structure has an evident impact on the transmission window and the leakage loss [34]. We also observed higher-order modes in the negative curvature fibers [35].

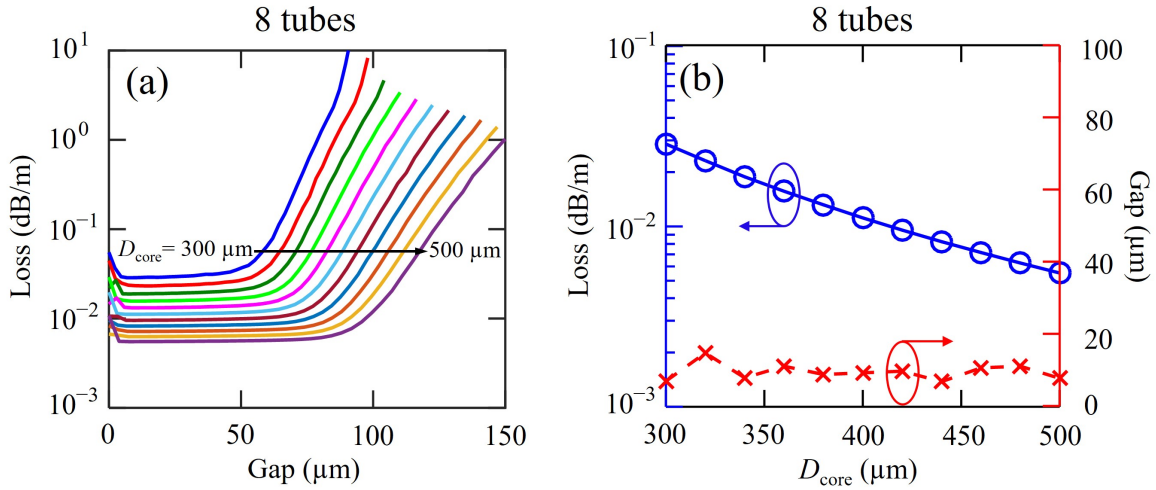

Figure 8. (**a**) Loss as a function of gap in fibers with different core diameters. (**b**) Minimum loss and corresponding gap in fibers with different core diameters. The number of cladding tube is eight.

5. Conclusions

In this paper, we optimize the structure of negative curvature fibers for CO_2 laser transmission. We investigate the impact of the size of the gap between cladding tubes on the loss of negative curvature fibers made with As_2Se_3 and As_2S_3 chalcogenide glasses. For As_2Se_3 chalcogenide fibers with six cladding tubes, the minimum loss decreases by an order of magnitude and the corresponding optimum gap, g, increases from 60 to 90 μm when the core diameter increases from 300 to 500 μm. A greater gap is needed for a fiber with greater core diameter to reduce the coupling between the core mode and tube mode. For a fiber with eight cladding tubes, the optimum gap, g, that corresponds to the minimum loss is always less than 20 μm when the core diameter ranges from 300 to 500 μm. We also study As_2S_3 chalcogenide fibers, which has a higher material loss at a wavelength of 10.6 μm. It is found that material loss dominates the fiber leakage loss. The fiber loss is dominated by the material loss, when the material absorption loss is higher than 10^2 dB/m.

Author Contributions: Supervision, C.R.M. and J.H.; Validation, C.R.M. and J.H.; Writing: original draft, C.W.; Writing: review and editing, C.W., C.R.M. and J.H.

Funding: Work at Baylor was supported by the National Science Foundation (ECCS-1809622). Work at UMBC was supported by the Naval Research Laboratory.

Conflicts of Interest: The authors declare no conflict of interest.

References

1. Snakenborg, D.; Klank, H.; Kutter, J.P. Microstructure fabrication with a CO_2 laser system. *J. Micromech. Microeng.* **2004**, *14*, 182–189. [CrossRef]
2. Hædersdal, M.; Sakamoto, F.H.; Farinelli, W.A.; Doukas, A.G.; Tam, J.; Anderson, R.R. Fractional CO_2 laser-assisted drug delivery. *Lasers Surg. Med.* **2010**, *42*, 113–122. [CrossRef] [PubMed]
3. Witteman, W.J. *The CO_2 Laser*; Enoch, J.F., Macadam, D.L., Schawlow, A.L., Shimoda, K., Tamir, T., Eds.; Springer: Berlin, Germany, 1987; pp. 1–4, ISBN 978-3-540-47744-0.
4. Poletti, F.; Petrovich, M.N.; Richardson, D.J. Hollow-core photonic bandgap fibers: Technology and applications. *Nanophotonics* **2013**, *2*, 315–340. [CrossRef]
5. Roberts, P.J.; Couny, F.; Sabert, H.; Mangan, B.J.; Williams, D.P.; Farr, L.; Mason, M.W.; Tomlinson, A.; Birks, T.A.; Knight, J.C.; et al. Ultimate low loss of hollow-core photonic crystal fibres. *Opt. Express* **2005**, *13*, 236–244. [CrossRef] [PubMed]

6. Wang, Y.Y.; Couny, F.; Roberts, P.J.; Benabid, F. Low loss broadband transmission in optimized core-shaped Kagome hollow-core PCF. In Proceedings of the Lasers Electro-Optics, Quantum Electron, Laser Science Conference, San Jose, CA, USA, 16–21 May 2010.
7. Wang, Y.Y.; Wheeler, N.V.; Couny, F.; Roberts, P.J.; Benabid, F. Low loss broadband transmission in hypocycloid-core Kagome hollow-core photonic crystal fiber. *Opt. Lett.* **2011**, *36*, 669–671. [CrossRef] [PubMed]
8. Pryamikov, A.D.; Biriukov, A.S.; Kosolapov, A.F.; Plotnichenko, V.G.; Semjonov, S.L.; Dianov, E.M. Demonstration of a waveguide regime for a silica hollow-core microstructured optical fiber with a negative curvature of the core boundary in the spectral region >3.5 μm. *Opt. Express* **2011**, *19*, 1441–1448 . [CrossRef] [PubMed]
9. Yu, F.; Wadsworth, W.J.; Knight. J.C. Low loss silica hollow core fibers for 3–4 μm spectral region. *Opt. Express* **2012**, *20*, 11153–11158. [CrossRef] [PubMed]
10. Wei, C.; Weiblen, R.J.; Menyuk, C.R.; Hu, J. Negative curvature fibers. *Adv. Opt. Photon.* **2017**, *9*, 504–561. [CrossRef]
11. Michieletto, M.; Lyngs, J.K.; Jakobsen, C.; Lgsgaard, J.; Bang, O.; Alkeskjold, T.T. Hollow-core fibers for high power pulse delivery. *Opt. Express* **2016**, *24*, 7103–7119. [CrossRef] [PubMed]
12. Wei, C.; Menyuk, C.R.; Hu, J. Polarization-filtering and polarization-maintaining low-loss negative curvature fibers. *Opt. Express* **2018**, *26*, 9528–9540. [CrossRef] [PubMed]
13. Kosolapov, A.F.; Pryamikov, A.D.; Biriukov, A.S.; Shiryaev, V.S.; Astapovich, M.S.; Snopatin, G.E.; Plotnichenko, V.G.; Churbanov, M.F.; Dianov, E.M. Demonstration of CO_2-laser power delivery through chalcogenide glass fiber with negative-curvature hollow core. *Opt. Express* **2011**, *19*, 2572–25728. [CrossRef] [PubMed]
14. Shiryaev, V.S. Chalcogenide glass hollow-core microstructured optical fibers. *Front. Mater.* **2015**, *2*, 24. [CrossRef]
15. Gattass, R.R.; Rhonehouse, D.; Gibson, D.; McClain, C.C.; Thapa, R.; Nguyen, V.Q.; Bayya, S.S.; Weiblen, R.J.; Menyuk, C.R.; Shaw, L.B.; et al. Infrared glass-based negative-curvature anti-resonant fibers fabricated through extrusion. *Opt. Express* **2016**, *14*, 25697–25703 . [CrossRef] [PubMed]
16. Wei, C.; Hu, J.; Menyuk, C.R. Comparison of loss in silica and chalcogenide negative curvature fibers as the wavelength varies. *Front. Phys.* **2016**, *4*, 30. [CrossRef]
17. Debord, B.; Amsanpally, A.; Chafer, M.; Baz, A.; Maurel, M.; Blondy, J.M.; Hugonnot, E.; Scol, F.; Vincetti, L.; Gérôme, F.; et al. Ultralow transmission loss in inhibited-coupling guiding hollow fibers. *Optica* **2017**, *4*, 209–217 . [CrossRef]
18. Debord, B.; Alharbi, M.; Bradley, T.; Fourcade-Dutin, C.; Wang, Y.Y.; Vincetti, L.; Gérôm, F.; Benabid, F. Hypocycloid-shaped hollow-core photonic crystal fiber Part I: Arc curvature effect on confinement loss. *Opt. Express* **2013**, *21*, 28597–28608. [CrossRef] [PubMed]
19. Yu, F.; Knight, J.C. Negative curvature hollow-core optical fiber. *IEEE J. Sel. Top. Quantum Electron.* **2016**, *22*, 4400610. [CrossRef]
20. Hu, J.; Menyuk, C.R. Understanding leaky modes: Slab waveguide revisited. *Adv. Opt. Photonics* **2009**, *1*, 58–106. [CrossRef]
21. Alagashev, G.K.; Pryamikov, A.D.; Kosolapov, A.F.; Kolyadin, A.N.; Lukovkin, A.Y.; Biriukov, A.S. Impact of geometrical parameters on the optical properties of negative curvature hollow core fibers. *Laser Phys.* **2015**, *25*, 055101. [CrossRef]
22. Poletti, F. Nested antiresonant nodeless hollow core fiber. *Opt. Express* **2014**, *22*, 23807–23828. [CrossRef] [PubMed]
23. Habib, M.S.; Bang, O.; Bache, M. Low-loss hollow-core silica fibers with adjacent nested anti-resonant tubes. *Opt. Express* **2015**, *23*, 17394–17406. [CrossRef] [PubMed]
24. Belardi, W.; Knight, J.C. Hollow antiresonant fibers with reduced attenuation. *Opt. Lett.* **2014**, *39*, 1853–1856. [CrossRef] [PubMed]
25. Kolyadin, A.N.; Kosolapov, A.F.; Pryamikov, A.D.; Biriukov, A.S.; Plotnichenko, V.G.; Dianov, E.M. Light transmission in negative curvature hollow core fiber in extremely high material loss region. *Opt. Express* **2013**, *21*, 9514–9519. [CrossRef] [PubMed]
26. Wei, C.; Menyuk, C.R.; Hu, J. Impact of cladding tubes in chalcogenide negative curvature fibers. *IEEE Photonics J.* **2016**, *8*, 2200509. [CrossRef]

27. Uebel, P.; Günendi, M.C.; Frosz, M.H.; Ahmed, G.; Edavalath, N.N.; Ménard, J.-M.; Russell, P.S.J. Broadband robustly single-mode hollow-core PCF by resonant filtering of higher-order modes. *Opt. Lett.* **2016**, *41*, 1961–1964. [CrossRef] [PubMed]
28. Liu, X.; Ding, W.; Wang, Y.Y.; Gao, S.; Cao, L.; Feng, X.; Wang, P. Characterization of a liquid-filled nodeless anti-resonant fiber for biochemical sensing. *Opt. Lett.* **2017**, *42*, 863–866. [CrossRef] [PubMed]
29. Wei, C; Menyuk, C.R.; Hu, J. Bending-induced mode non-degeneracy and coupling in chalcogenide negative curvature fibers. *Opt. Express* **2016**, *24*, 12228–12239. [CrossRef] [PubMed]
30. Saitoh, K.; Koshiba, M. Leakage loss and group velocity dispersion in air-core photonic bandgap fibers. *Opt. Express* **2003**, *11*, 3100–3109. [CrossRef] [PubMed]
31. Caillaud, C.; Renversez, G.; Brilland, L.; Mechin, D.; Calvez, L.; Adam, J.-L.; Troles, J. Photonic Bandgap Propagation in All-Solid Chalcogenide Microstructured Optical Fibers. *Materials* **2014**, *7*, 6120–6129. [CrossRef] [PubMed]
32. Wei, C.; Kuis, R.A.; Chenard, F.; Menyuk, C.R.; Hu, J. Higher-order mode suppression in chalcogenide negative curvature fibers. *Opt. Express* **2015**, *23*, 15824–15832. [CrossRef] [PubMed]
33. Belardi, W.; Knight, J.C. Negative curvature fibers with reduced leakage loss. In Proceedings of the Optical Fiber Communication Conference, San Francisco, CA, USA, 9–13 March 2014.
34. Weiblen, R.J.; Menyuk, C.R.; Gattass, R.R.; Shaw, L.B.; Sanghera, J.S. Fabrication tolerances in As_2S_3 negative-curvature antiresonant fibers. *Opt. Lett.* **2016**, *41*, 2624–2627. [CrossRef] [PubMed]
35. Hayes, J.R.; Sandoghchi, S.R.; Bradley, T.D.; Liu, Z.; Slavik, R.; Gouveia, M.A.; Wheeler, N.V.; Jasion, G.; Chen, Y.; Fokoua, E.N.; et al. Antiresonant hollow core fiber with an octave spanning bandwidth for short haul data communications. *J. Lightw. Technol.* **2017**, *35*, 437–442. [CrossRef]

© 2018 by the authors. Licensee MDPI, Basel, Switzerland. This article is an open access article distributed under the terms and conditions of the Creative Commons Attribution (CC BY) license (http://creativecommons.org/licenses/by/4.0/).